IEEE Access
Multidisciplinary | Rapid Review | Open Access Journal

Received December 17, 2020, accepted December 29, 2020, date of publication January 8, 2021, date of current version January 14, 2021.

Digital Object Identifier 10.1109/ACCESS.2021.3049768

Assessing the Feasibility of Game-Theory-Based Demand Response Management by Practical Implementation

MENGMENG YU[1], (Member, IEEE), XIONGFENG ZHANG[1], JUNHUI JIANG[1], (Graduate Student Member, IEEE), CHANGDAE LEE[1], (Student Member, IEEE), SEUNG HO HONG[1], (Senior Member, IEEE), KAI WANG[2,3], AND AIDONG XU[2,3]

[1]Department of Electronic Engineering, Hanyang University, Ansan 15588, South Korea
[2]Key Laboratory of Networked Control Systems, Chinese Academy of Science, Shenyang Institute of Automation, Shenyang 110016, China
[3]Institutes for Robotics and Intelligent Manufacturing, Chinese Academy of Sciences, Shenyang 110169, China

Corresponding author: Seung Ho Hong (shhong@hanyang.ac.kr)

This work was supported in part by the framework of international cooperation program managed by the National Research Foundation of Korea under Grant NRF-2018K1A3A1A61026340, and in part by the Human Resources Program in Energy Technology of the Korea Institute of Energy Technology Evaluation and Planning (KETEP), granted financial resource from the Ministry of Trade, Industry and Energy under Grant 20174030201780.

ABSTRACT Demand response (DR) has been widely recognized as an effective solution to help mitigate the stresses imposed on power grids. As new concepts evolve, DR induces various interactions among multiple emerging entities, which further complicates the decision-making processes in grid operations. Recently, game theory (GT) has received great attention in DR management, due to its ability to handle complex decision-making problems. Numerous theoretical GT-based approaches have been proposed for addressing various DR issues, but the feasibility of these theoretical approaches in practical implementation remains in doubt. To bridge the gap between theoretical studies and practical implementations, we first provide specific guidelines regarding how to construct a DR-oriented facility, and then investigate the effectiveness of deploying a Stackelberg game theory-based DR algorithm to manage the energy consumption of the facility, wherein the energy management center (EMC) serves as the leader and multiple devices act as the followers. The experimental evaluation results show that the GT-based DR algorithm achieved great performance in practical DR management, including optimal load control in responding to real-time price (RTP), and peak load reduction with a peak-to-average ratio (PAR) of 1.59.

INDEX TERMS Demand response (DR), implementation, energy management, game theory.

NOMENCLATURE

ACRONYMS

DR	Demand response
EMC	Energy management center
GT	Game theory
GUI	Graphical user interface
PAR	Peak-to-average ratio
RTP	Real-time price
SE	Stackelberg Equilibrium
TSN	Time sensitive networking
VRP	Virtual retail price

The associate editor coordinating the review of this manuscript and approving it for publication was Lei Wang.

INDICES AND SETS

i	Index for device
$\boldsymbol{I}_{\text{con}}$	Set of continuous type of devices
$\boldsymbol{I}_{\text{dis}}$	Set of discrete type of devices
N	Total number of devices, $N = \lvert \boldsymbol{I}_{\text{con}} \rvert + \lvert \boldsymbol{I}_{\text{dis}} \rvert$

FUNCTIONS AND VARIABLES

x_i	Energy demand (Wh) or decision variable of device i
c_i	Virtual retail price (cents/kWh) for device i
$\varphi_i(\cdot)$	Dissatisfaction cost function for device i
$\mathrm{U}_i(\bar{\mathbf{c}}, x_i)$	Objective function of device i

$U_{EMC}(\bar{\mathbf{c}}, \bar{\mathbf{x}})$	Objective function of EMC
$(\bar{\mathbf{c}}^*, \bar{\mathbf{x}}^*)$	Stackelberg equilibrium (SE)
$\bar{\mathbf{c}} = [c_1, c_2, \ldots, c_N]$	Virtual retail price vector
$\bar{\mathbf{x}}^* = [x_1^*, x_2^*, \ldots, x_N^*]$	Optimal control strategy for N devices

PARAMETERS

C_{RTP}	Real-time price (cents/kWh) received from utility
$x_i^{\min}, x_i^{\max}$	Minimal and maximal energy demand ranges (Wh) for a continuous type device
m_i	Median level of energy demand (Wh) for a continuous type device
x_i^{nom}	Nominal energy (Wh) of a discrete type device
τ_i	Threshold used to determine the operation of a discrete device ($0 \leq \tau_i \leq 1$)
β_i	Priority of a device
ω	Weighting factor that incorporates the significance of user satisfaction

I. INTRODUCTION

The ever-increasing demand for electricity and the growing penetration of intermittent renewable energy sources pose severe challenges to power grids in maintaining real-time balance between demand and supply [1]. In recent decades, demand response (DR), which aims to explore the inherent flexibility of the demand side, has been widely regarded as an effective and powerful means to meet those challenges [2], [3]. In general, DR is envisaged to both help improve the overall operation efficiency and reliability of smart grids [4], and benefit consumers in certain ways.

Existing DR mechanisms can be generally classified into two categories. The first allows the utility company to control consumers' loads directly [5], which provides great flexibility to the system operator, but compels consumers to give up control over managing their energy consumption based on their own preferences [6]. The second category of DR reshapes loads through dynamic pricing schemes such as real-time pricing (RTP), under which electricity prices vary from hour to hour [7], and consumers are expected to respond to the price signal by shifting loads from peak hours to off-peak hours [8]. RTP is further categorized into two kinds of pricing scheme depending on the price updating cycle, i.e., day-ahead RTP in which hourly retail prices are set one day ahead of the actual consumption, and hour-ahead RTP in which a new price is announced for each upcoming hour [9].

In recent years, numerous studies have been conducted on devising RTP-based DR approaches oriented for either residential [10], [11], commercial [12], [13] or industrial consumers [14], [15]. Among those existing approaches, game theory (GT) has attracted great attention for modeling complex interactions between various entities under a DR framework [10], [11], [16], since GT has been proven to be an effective tool for solving many challenging real-world problems and handling complex decision-making processes [17]. For instance, a Stackelberg game based energy management framework was proposed in [18] for joint operation of combined heat and power and photovoltaic prosumers. The work in [19] proposed a bargaining-based cooperative game to solve the irreconcilable pricing problem of multiple aggregators with overlapping consumers. In work [20], a game theoretical-based incentivizing strategy was proposed to help a demand response aggregator determine the optimal incentive for each customer based on their identified characteristics. The study in [21] applied game theory to model a hierarchical system in which multiple providers and prosumers competed with each other to determine the optimal energy price and demand. Jiang *et al.* [22] proposed a game-theory based pricing model among prosumers in an energy blockchain environment, where the interactions between seller and buyer as well as the interactions among sellers were considered.

The superiority of applying GT to address smart grid or DR problems has already been verified theoretically through the studies highlighted above, as well as other extensive publications. However, most of those approaches were verified using simulation without deploying real devices, implying that customers are actually not aware how to implement those approaches in reality. To the best of our knowledge, scarce works took the practical viewpoint to provide guidelines for implementing DR approaches (especially those GT-based approaches) in practice. Recently, one latest paper [23] has made a breakthrough from a practical aspect by devising a web-based platform, over which an application programming interface (API) was developed to guide users how to acquire and process DR related data. However, the DR approach in [23] was also verified using simulation, which means the applicability of this platform is constrained as the cloud service.

In light of this gap between theoretical studies and practical deployment, this study examined the effectiveness of deploying a GT-based DR algorithm for managing the energy consumption of a diversified facility in the context of a price-based DR environment. Specifically, we constructed a practical experimental facility equipped with a range of hardware and software; the details are specified in later sections. Over the constructed experimental facility, a typical GT-based DR algorithm was implemented to assess the performance of real-time energy management of various field devices. The experimental evaluation results show that the GT-based DR algorithm was effective for DR management in practice, including optimal load control, peak load reduction, etc.

To the best of our knowledge, this is the first study showing a specific procedure for deploying a GT-based DR approach in a real-world facility, which tactfully fills the gap between theoretical studies and practical implementations. Moreover, since interactions between different participants within the energy system are becoming inevitable, this work can be regarded as a proof of concept in guiding how other GT

approaches could be put into practice and can also encourage more researches to be conducted in this area by exploiting game theory. To this end, the main contributions of this paper are:

- First, different with existing theoretical approaches, this paper takes one step forward that aims to fill the gap between theoretical studies and practical implementations by demonstrating a real application of game theory-based decision making approach through an experimental setup.
- Second, in this pioneering work, a DR-oriented experimental facility was constructed by specifying all key technical details from cloud-based user interface to hardware-based deployment of end devices, which is believed to be a prominent progress in the industry sector.
- Third, in addition to constructing the experimental facility, we provide guidelines to demonstrate the procedure for implementing a typical GT-based DR algorithm to evaluate the feasibility of a game-theoretic approach in practical DR implementation and assess the effectiveness of managing the real-time energy consumption of various field devices in response to hourly RTP.
- Fourth, the experimental evaluation results verify that the GT-based DR algorithm achieved excellent performance in practical DR management, which sheds light on more extensive implementations of other advanced GT-related DR approaches in diversified DR applications.

The remainder of this paper is organized as follows. Section II briefly introduces the adopted GT-based DR algorithm. In Section III, we present the system structure and experimental facility setup of the proposed demand-response management system. Section IV discusses the experimental evaluation results, and Section V provides conclusions and future work.

II. KEY PRINCIPLES OF THE GAME THEORY (GT)-BASED DEMAND-RESPONSE (DR) ALGORITHM

The GT-based DR algorithm proposed in [24] was adopted to manage the energy consumption of diversified devices in a facility in the context of a price-based DR environment. It deserves noticing that the DR approach adopted in this paper is just an example, we leave users the freedom to choose any desirable DR approach to be deployed, or one user may even reserve different DR approaches and then deploy the most beneficial one according to the real-time DR signal or user preference.

In this section, the key principles of the GT-based DR algorithm [24] are summarized. In general, the algorithm is oriented to a facility equipped with an energy management center (EMC) that receives the real-time price (RTP) from the utility company periodically (e.g., hourly). In response to the received RTP, the EMC is responsible for determining the optimal control strategy to manage the energy consumption of a number of N various devices (continuous and discrete types). To achieve this, a virtual electricity-trading process is establi-shed between the EMC and the devices, and Stackelberg GT is adopted to model the trading procedure, due to its superiority in solving hierarchical decision-making problems [25].

Consider that there are multiple devices (followers), accordingly, an 1-leader, N-follower Stackelberg game is formulated with EMC being the leader who offers virtual retail prices (VRPs) to devices (followers), and each device reacts to the VRP by demanding energy from the EMC. Next, the mathematical models of each engaged entity as well as the Stackelberg representation are summarized as follows.

A. DEVICE (FOLLOWER) MODEL

Two types of devices are considered in the model: continuous and discrete energy-consumption, denote $\boldsymbol{I}_{\text{con}}$ and $\boldsymbol{I}_{\text{dis}}$ respectively. When notified by the VRPs ($\bar{\mathbf{c}} = [c_1, c_2, \ldots, c_N]$) from the EMC, a device i aims to determine its optimal energy demand (x_i) by solving its optimization problem defined as follows:

$$\min_{x_i} \mathrm{U}_i(\bar{\mathbf{c}}, x_i) = \begin{cases} c_i \cdot x_i + \omega \cdot \varphi_i(x_i) & i \in \boldsymbol{I}_{\text{con}} \quad (1a) \\ c_i \cdot x_i \cdot x_i^{nom} + \omega \cdot \varphi_i(x_i) & i \in \boldsymbol{I}_{\text{dis}} \quad (1b) \end{cases}$$

$$s.t.\ x_i^{\min} \le x_i \le x_i^{\max} \quad i \in \boldsymbol{I}_{\text{con}} \quad (1c)$$

$$0 \le x_i \le 1 \quad i \in \boldsymbol{I}_{\text{dis}} \quad (1d)$$

On the right side of (1a) and (1b), the first term represents the virtual monetary cost of purchasing energy from the EMC and the second term denotes the dissatisfaction cost $\varphi_i(\cdot)$, which evaluates the dissatisfaction level of a device, where x_i^{nom} denotes the nominal energy of discrete type device i, and ω is a weighting factor that incorporates the significance of user satisfaction over a given period. (1c) and (1d) provide the minimal and maximal ranges for continuous type and discrete type devices respectively. The method of how to convert the binary decision variable of a discrete type device into a real-valued variable will be introduced later on.

The specific form of the dissatisfaction cost function $\varphi_i(\cdot)$ is provided in (2) [24], where β_i indicates the priority of each device i (a smaller value of β_i represents higher priority, and vice versa), and $m_i = \frac{(x_i^{\min} + x_i^{\max})}{2}$ in (2a) denotes the median level of energy demand, τ_i in (2b) is a threshold ($0 \le \tau_i \le 1$) used to determine the operation of a discrete device.

$$\varphi_i(x_i) = \begin{cases} e^{\beta_i\left(1-(\frac{x_i}{m_i})\right)} - 1, \ \beta_i > 0 & i \in \boldsymbol{I}_{\text{con}} \quad (2a) \\ e^{\beta_i\left(1-(\frac{x_i}{\tau_i})\right)} - 1, \ \beta_i > 0\ 0 \le \tau_i \le 1 & i \in \boldsymbol{I}_{\text{dis}} \quad (2b) \end{cases}$$

For a discrete type device $i \in \boldsymbol{I}_{\text{dis}}$, its discrete decision variable x_i (0 or 1) in (1b) and (1d) can be transformed into a real value variable ($0 \le x_i \le 1$) [24]. Note that minimizing (2b) indicates the value of function $\varphi_i(\cdot)$ is approaching to zero, which further means the value of x_i is enforced to be approaching to τ_i. Throughout this paper, τ_i is set to be

one, in this way we can get a binary solution for the original discrete problem by rounding x_i to one, when x_i is equal to or greater than one. More explanations can be found from Part *D* of this section by referring to the optimization process.

B. EMC (LEADER) MODEL

The EMC aims to maximize its virtual benefit through trading with devices, while also taking into account the dissatisfaction costs of devices. The objective function of the EMC is formulated in (3), through which the optimal VRPs ($\bar{\mathbf{c}} = [c_1, c_2, \ldots, c_N]$) can be determined.

$$\max_{\bar{\mathbf{c}}} \mathrm{U}_{EMC}(\bar{\mathbf{c}}, \bar{\mathbf{x}}) = \sum_{i=1}^{N} c_i x_i - \sum_{i=1}^{N} \omega \cdot \varphi_i(x_i) \quad (3a)$$

$$s.t. \sum_{i=1}^{N} c_i = C_{RTP} \quad (3b)$$

$$0 < c_i < C_{RTP} \text{ for } i = 1, \ldots, N \quad (3c)$$

where N denotes the total number of devices, i.e., $N = |\boldsymbol{I}_{\mathrm{con}}| + |\boldsymbol{I}_{\mathrm{dis}}|$. Equation (3b) constrains that the sum of VRPs should be equal to the RTP (C_{RTP}), which is supposed to be periodically received from the utility, and each VRP (c_i) for device i is constrained by (3c). Accordingly, VRPs for each device would vary every hour, reflecting the dynamic changes of RTP.

C. GAME FORMULATION BETWEEN EMC (LEADER) AND DEVICES (FOLLOWERS)

To help understand how a 1-leader, N-follower Stackelberg game is formulated between an EMC and devices (given above mathematical models), the gaming process has been briefly summarized in Appendix A.

D. OUTPUT FROM THE GT-BASED DR ALGORITHM

Regarding the gaming process illustrated in Part *C*, the desired outcome takes the form of Stackelberg Equilibrium (SE), which can be regarded as the output from the GT-based DR algorithm. Mathematically, the SE is a profile of strategies ($\bar{\mathbf{c}}^*, \bar{\mathbf{x}}^*$) that corresponds to the solution of the following nested optimization problems [24], [25].

$$(\bar{\mathbf{c}}^*, \bar{\mathbf{x}}^*) = \arg \max_{(\bar{\mathbf{c}}, \bar{\mathbf{x}}) \in \Omega_{EMC} \times \Omega_i} U_{EMC}(\bar{\mathbf{c}}, \bar{\mathbf{x}}^*) \quad (4a)$$

$$s.t. x_i^* = \arg \min_{\mathbf{x}_i \in \Omega_i} \mathrm{U}_i(\bar{\mathbf{c}}, x_i) \quad \forall i \in \boldsymbol{I}_{\mathrm{con}} \cup \boldsymbol{I}_{\mathrm{dis}} \quad (4b)$$

To help better understand the optimization process of the control scheme, in Table 1 we have summarized the key steps for deriving the SE by solving the nested optimization problem in (4), and the details are provided as follows:

From line 1 to line 4, we apply backward induction principle to identify the best-response strategy for each device by solving (4b). Note that solving (4b) is equivalent to solving (1a) and (1b). As such, by taking the first-order derivative of (1a) and (1b), we can get the best response functions in terms of (5a) and (5b) for continuous type device and discrete type device, respectively.

From line 5 to line 11, new VRP (c_i) constraints are derived for the EMC based on the best response functions

TABLE 1. Key Steps of GT-based DR Algorithm Optimization.

	Key steps for deriving the SE ($\bar{\mathbf{c}}^*, \bar{\mathbf{x}}^*$) :
1:	**Identify best-response strategy for each device by solving (4b) [24]:**
2:	Obtain (5a) and (5b) by taking the first-order derivative of (1) [24]).
3:	For continuous type: $x_i(\bar{\mathbf{c}}) = m_i(1 - \frac{1}{\beta_i} \ln \frac{c_i m_i}{\omega \beta_i})$ (5a)
4:	For discrete type: $x_i(\bar{\mathbf{c}}) = \tau_i(1 - \frac{1}{\beta_i} \ln \frac{c_i x_i^{nom} \tau_i}{\omega \beta_i})$ (5b)
5:	**Derive new VRP (c_i) constraints for EMC [24]:**
6:	Inversely rewrite (5a) and (5b) as two decreasing functions of x_i:
7:	For continuous type: $c_i(x_i) = \frac{\omega \beta_i}{m_i} e^{\beta_i (1 - \frac{x_i}{m_i})}$ (6a)
8:	For discrete type: $c_i(x_i) = \frac{\omega \beta_i}{x_i^{nom} \tau_i} e^{\beta_i (1 - \frac{x_i}{\tau_i})}$ (6b)
9:	Determine new VRP constraints according to (1c), (1d) and (3c):
10:	For continuous type: $\frac{\omega \beta_i}{m_i} e^{\beta_i (1 - \frac{x_i^{\min}}{m_i})} \le c_i \le \min\left\{ \frac{\omega \beta_i}{m_i} e^{\beta_i (1 - \frac{x_i^{\min}}{m_i})}, C_{RTP} \right\}$ (7a)
11:	For discrete type: $\frac{\omega \beta_i}{x_i^{nom} \tau_i} e^{\beta_i (1 - \frac{1}{\tau_i})} \le c_i \le \min\left\{ \frac{\omega \beta_i}{x_i^{nom} \tau_i} e^{\beta_i}, C_{RTP} \right\}$ (7b)
12:	**Reformulate EMC optimization problem by substituting (5a) and (5b) into (4a):**
13:	$\max_{\bar{\mathbf{c}}} \mathrm{U}_{EMC}(\bar{\mathbf{c}}, \bar{\mathbf{x}}) = \sum_{i=1}^{\lvert I_{\mathrm{con}} \rvert} \left(c_i \cdot m_i (1 - \frac{1}{\beta_i} \ln \frac{c_i m_i}{\omega \beta_i}) \right) - \sum_{i=1}^{\lvert I_{\mathrm{con}} \rvert} \left(\frac{c_i m_i}{\beta_i} - \omega \right)$ $+ \sum_{j=1}^{\lvert I_{\mathrm{dis}} \rvert} \left(c_j \cdot \tau_j (1 - \frac{1}{\beta_j} \ln \frac{c_j x_j^{nom} \tau_j}{\omega \beta_j}) \right) - \sum_{j=1}^{\lvert I_{\mathrm{dis}} \rvert} \left(\frac{c_j x_j^{nom} m_j}{\beta_j} - \omega \right)$ (8a)
14:	*s.t.* (3b), (7a) and (7b) (8b)
15:	**Solve (8) using commercial software to obtain the unique and optimal VRP vector ($\bar{\mathbf{c}}^* = [c_1^*, c_2^*, \ldots, c_N^*]$) for EMC.**
16:	Determine optimal energy demand (x_i^*) and optimal decision variable (x_i^*) for each continuous and discrete device by substituting ($\bar{\mathbf{c}}^* = [c_1^*, c_2^*, \ldots, c_N^*]$) back into (5a) and (5b), respectively.
17:	**Ascertain SE ($\bar{\mathbf{c}}^*, \bar{\mathbf{x}}^*$) based on the optimal results in lines 15 and 16.**

in (5a) and (5b). Specifically, we first inversely rewrite (5a) and (5b) as two decreasing functions of x_i as illustrated in (6a) and (6b). Afterwards, new VRP (c_i) constraints can be determined by substituting the lower and upper bounds of (1c) and (1d) into (6a) and (6b), respectively. Moreover, by conjunctively considering the original VRP constraint in (3c), we can finally determine the new VRP constraints as expressed in (7a) and (7b).

From line 12 to line 14, according to the backward induction principle, the original EMC optimization problem is readily to be reformulated. We first rewrite the objective function of EMC by substituting (5a) and (5b) into (4a), where (4a) is equivalent to (3a). In accordance, we can get the updated EMC objective function in the form of (8a). To this end, the EMC optimization problem can be reformulated into (8a) and (8b). In Appendix B, we have proven that the reformulated optimization problem is a strictly convex problem, which means a unique and optimal solution is guaranteed. In other words, a unique and optimal VRP vector ($\bar{\mathbf{c}}^* = [c_1^*, c_2^*, \ldots, c_N^*]$) can be obtained by solving (8).

From line 15 to line 16, we emphasize that the reformulated EMC problem in (8) can be solved using commercial software, in order to obtain the unique and optimal VRP vector ($\bar{\mathbf{c}}^* = [c_1^*, c_2^*, \ldots, c_N^*]$). Afterwards, we can determine the optimal energy demand (x_i^*) for each continuous type device by substituting ($\bar{\mathbf{c}}^* = [c_1^*, c_2^*, \ldots, c_N^*]$) back into (5a), and

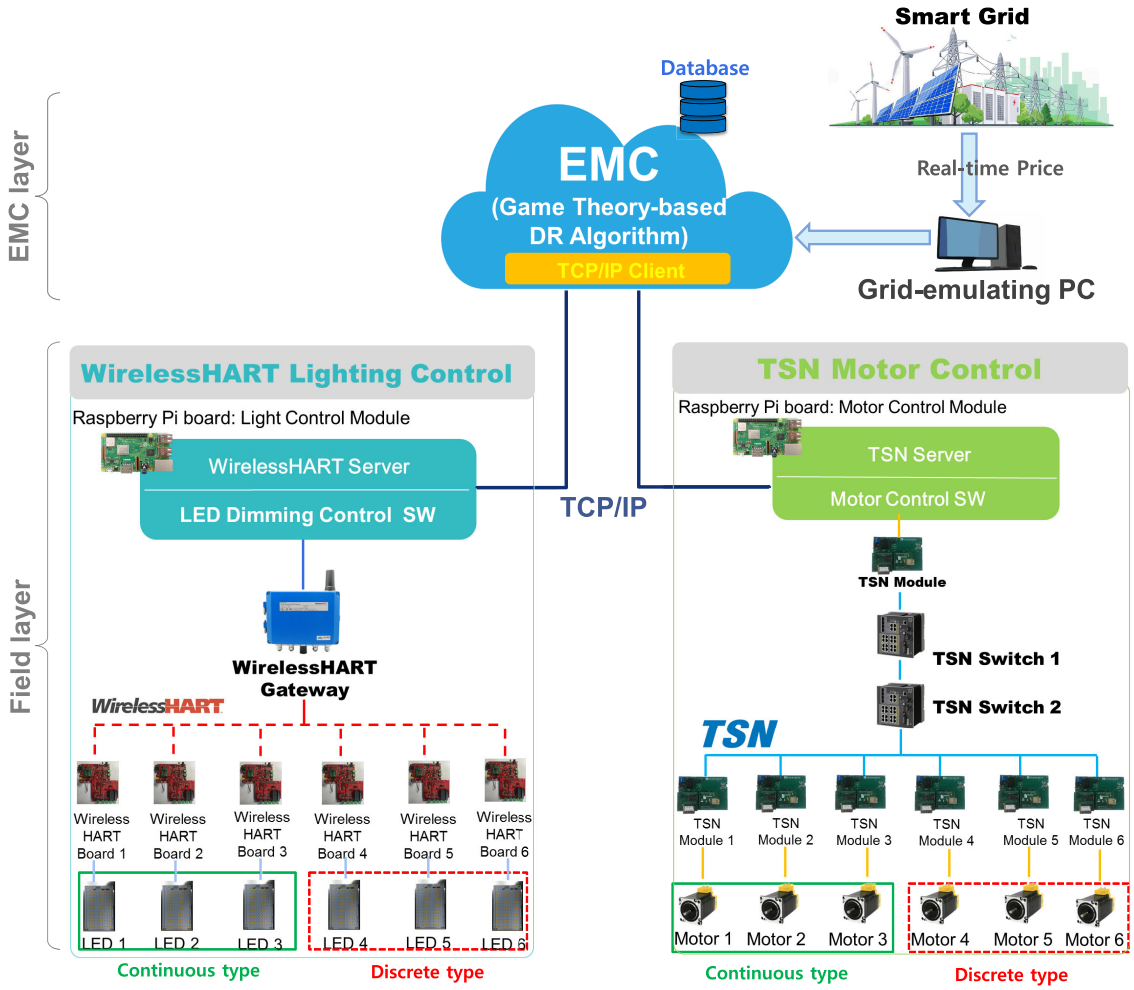

FIGURE 1. System architecture of the DR management system.

also determine the optimal decision variable (x_i^*) for each discrete type device by substituting ($\bar{\mathbf{c}}^* = [c_1^*, c_2^*, \ldots, c_N^*]$) back into (5b). In this way, we finally get the vector ($\bar{\mathbf{x}}^* = [x_1^*, x_2^* \ldots, x_N^*]$) containing the optimal energy demand and optimal decision variable for all the devices. Suppose x_i^* is the obtained optimal decision variable for a discrete device i in a given hour, if x_i^* is equal to or greater than τ_i, then we round x_i^* to one, indicating that device i is able to demand the full nominal energy (x_i^{nom}) during this hour. By doing this, we can obtain a binary solution for the original discrete problem, i.e., the "on" and "off" states can be determined accordingly.

In line 17, we conclude that the SE ($\bar{\mathbf{c}}^*, \bar{\mathbf{x}}^*$) is ascertained based on the optimal results obtained in line 15 and line 16. Clearly, over the SE, the optimal control strategy ($\bar{\mathbf{x}}^* = [x_1^*, x_2^* \ldots, x_N^*]$) is ascertained as well, which will be applied for managing the energy consumption of field devices.

Note that the algorithm is dynamically executed each hour when the EMC receives a new RTP, in this way we can obtain hourly optimal control strategy.

III. SYSTEM ARCHITECTURE AND EXPERIMENTAL FACILITY SETUP OF THE DEMAND-RESPONSE MANAGEMENT SYSTEM

This section presents the system architecture of the demand-response management system by dividing it into two layers, i.e., the EMC layer and the field layer, as illustrated by Figure 1. Moreover, Figure 2 shows the corresponding experimental facility setup composed of all the relevant software and hardware. Next, the related technical details will be introduced from bottom to top.

A. FIELD LAYER

The field layer represents physical sites deployed with diverse application-oriented devices. To have an intuitive observation of each device, in the proposed system as shown in Figure 1, we adopt six LED lamps as a lighting facility and six motors as a machine operation facility to represent the field devices. Note that more devices can be deployed in an expanded facility, since the adopted GT-based DR algorithm can avoid

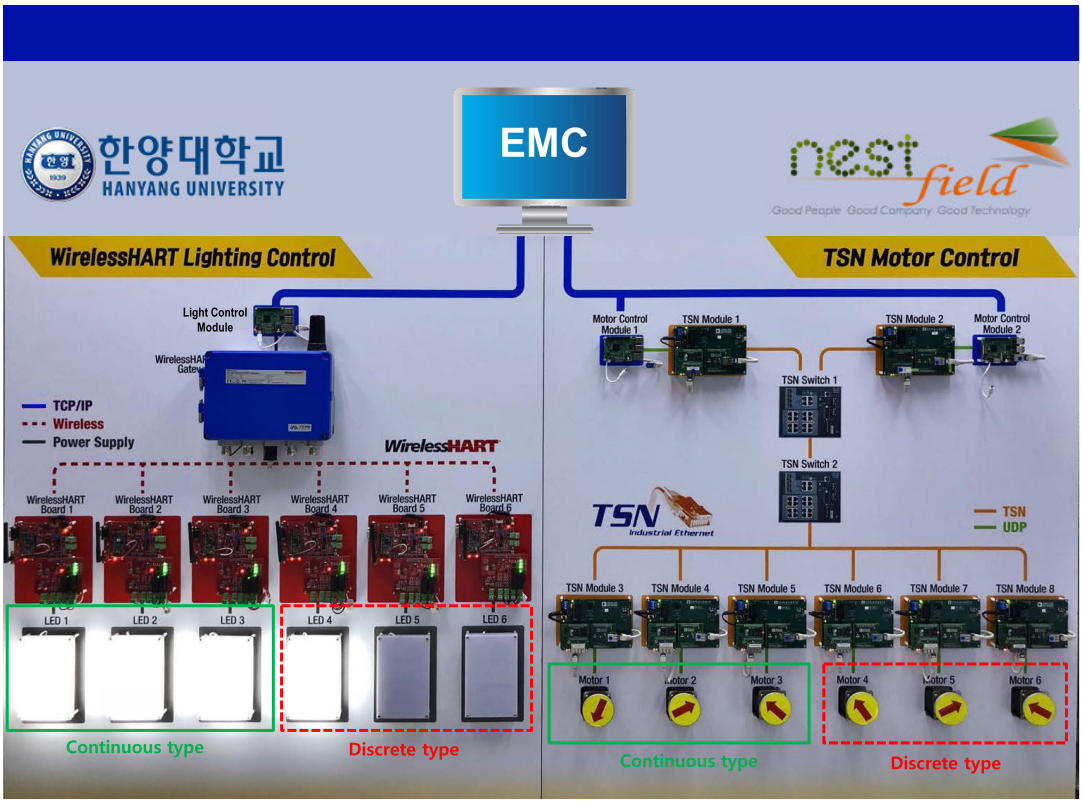

FIGURE 2. Experimental facility of GT-based DR management system.

iterations (refer to Appendix A) and thus is able to accommodate a number of devices. In the presented facility, three motors and three LED lamps are regarded as continuous-type devices, and the other three motors and three lamps are deemed discrete-type devices, with ''on'' and ''off'' states only.

It deserves noticing that there is no technical difference among six motors (lamps); in other words, all the motors (lamps) are physically same. In order to examine the effectiveness of GT-based algorithm, we artificially divided six motors (lamps) into three continuous types and three discrete types. Herein, ''continuous'' does not mean we change the power consumption of a device second by second or continuously. In our experimental system, a ''continuous type device'' means a device is always being on while controlling its power consumption within a min-max range. Moreover, we adjust the power consumption level of ''a continuous type lamp or motor'' every one hour when the real-time price is changed.

All the real devices are indicated in Figure 2, which shows the real-time operation status of each device. Note that the operation of each device is managed based on the commands (i.e., control strategy) received from the upper layer. Especially, we would like to clarify that in our experimental facility the ''on'' and ''off'' states of ''lamps'' and ''motors'' can be controlled directly, as the effect of thermal inertia for these two kinds of devices is negligible and thus can be neglected. Therefore, even though device thermal inertia was not considered in this paper, our experimental result has verified that it does not distort the DR management of the constructed facility.

Industrial communication networks are used to integrate these devices. In the present system, a WirelessHART network [26] and a time sensitive networking (TSN) network [27] are deployed for the lighting facility and the machine operation facility, respectively, in the field layer, representing typical wireless and wired industrial automation networks. To enable interconnectivity between the field layer and the EMC layer, the underlying TCP/IP servers (denoted as ''WirelessHART Server'' and ''TSN Server'' in Figure 1) together with the LED control software (and motor control software) were developed and implemented in Raspberry Pi boards [28], located on the edges of both field networks. For easier labelling, in the experimental facility shown in Figure 2, the TCP/IP servers and control software are named the ''Light Control Module'' and the ''Motor Control Module'', and used to bridge the WirelessHART gateway and the TSN modules to the EMC layer, to enable two main functionalities, i.e., LED dimming control and motor control. The ''Light Control Module'' and ''Motor Control Module'' execute the control strategy for energy consumption delivered from the EMC layer, and collect energy consumption data measured from the end devices. Other field networks can also be integrated into the system in a similar manner.

B. EMC LAYER

The EMC layer plays the key role of the established system in which the GT-based DR algorithm introduced in Section II is implemented. Next, we will first give an overall introduction of the DR participation process by referring to Figure 1, and then we specify details about how the GT-based DR algorithm is implemented and executed in the experimental facility.

As illustrated in Figure 1, the facility is supposed to be involved in an hour-ahead RTP-based DR program that receives a new price (¢/kWh) from the smart grid for each upcoming hour. In reality, there are already some service providers that are running this kind of RTP-based DR program by providing hourly real-time prices; one typical provider is the Commonwealth Edison Company (ComEd) [29]. To facilitate implementation in this experimental facility, a grid-emulating PC is set up to behave as the smart grid as illustrated in Figure 1. At the start of operation, this grid-emulating PC announces the RTP-based DR program to the EMC, and accordingly the EMC subscribes to the grid-emulating PC as an acknowledgement of participating in the proposed DR program. This subscription process can be done by means of deploying a grid server in the grid-emulating PC and an algorithm client in the EMC PC respectively. Note that as well as the mechanism proposed in this study, the OpenADR protocol [30] can also be deployed to realize communication between the grid side and the EMC, and users may choose either mechanism according to their preference. Upon establishing the connection, upon receipt of the RTP from the grid-emulating PC, the GT-based DR algorithm in the EMC is executed to determine the optimal control strategy ($\bar{\mathbf{x}}^* = [x_1^*, \ldots, x_N^*]$) for managing the energy consumption of field devices.

To better understand how the GT-based DR algorithm is implemented in the experimental facility, in Table 2 we have summarized the execution procedure into six steps, which specifies the actions that need to be executed to address different commands of Table 1. Next, more explanations will be provided with regard to each step of Table 2. In Step 1, the EMC is supposed to receive a new RTP (C_{RTP}) from the "grid-emulating PC" for the current hour, and then in Step 2 the EMC will first check whether the current stage is off-peak, middle peak or peak period, and then select the weight factor (ω) accordingly. Based on the input parameters provided by Table 3 and the weight factor selected in last step, in Step 3 the EMC will derive new VRP (c_i) constraints by executing the commands from line 5 to line 11 in Table 1. Afterwards, the EMC optimization problem will be reformulated as expressed in the form of problem (8) in Table 1. In Step 4, the EMC will execute the command of line 15 in Table 1 to solve the reformulated optimization problem. Specifically, the EMC will run Matlab toolbox "fmincon" (which is deemed as a commercial software) to obtain the unique and optimal VRP vector ($\bar{\mathbf{c}}^* = [c_1^*, c_2^*, \ldots, c_N^*]$). In Step 5, according to the obtained VRP vector, the EMC will determine the optimal energy demand (x_i^*) and optimal decision variable (x_i^*) for each continuous and discrete type device by executing the command of line 16 in Table 1. Finally, in Step 6 the EMC can ascertain the SE ($\bar{\mathbf{c}}^*$, $\bar{\mathbf{x}}^*$) based on the optimal results obtained in Step 4 and Step 5. In this manner, Step 1 to Step 6 will be repeated for each hour when a new RTP is received by the EMC.

TABLE 2. Execution of GT-based DR Algorithm.

Inputs:	device priority (β_i), weight factor (ω), minimum and maximum power rating ($x_i^{\min}, x_i^{\max}$), nominal energy demand (x_i^{nom}), threshold (τ_i)
Loop for each hour:	
Step 1:	EMC receives hourly RTP (C_{RTP}) from "grid-emulating PC".
Step 2:	Check the current stage (off-peak, middle peak or peak) and select weight factor (ω) accordingly.
Step 3:	Execute line 5-line 11 in Table I to derive new VRP (c_i) constraints.
Step 4:	Execute line 15 in Table I to solve the reformulated EMC optimization problem (8) using Matlab toolbox "fmincon" and obtain the unique and optimal VRP vector ($\bar{\mathbf{c}}^* = [c_1^*, c_2^*, \ldots, c_N^*]$) for EMC.
Step 5:	Execute line 16 in Table I to determine optimal energy demand (x_i^*) and optimal decision variable (x_i^*) for each continuous and discrete device.
Step 6:	Ascertain SE ($\bar{\mathbf{c}}^*, \bar{\mathbf{x}}^*$) based on the optimal results in Step 4 and Step 5.
Outputs:	Optimal control strategy ($\bar{\mathbf{x}}^* = [x_1^*, \ldots, x_N^*]$) for managing the energy consumption of field devices.

It deserves noticing that the EMC developed in our experimental system is cloud-based, through which the GT-based DR Algorithm can be accessed remotely to generate the optimal control strategy for managing the states of lamps and motors. In addition, to enable communication between the EMC layer and the field layer, an accompanying TCP/IP client is built into the EMC PC to serve as the communication interface to exchange information (i.e., dispatch the control strategy from top down, and receive the energy consumption data gathered from the field layer) using the WirelessHART server and the TSN server located on the Raspberry Pi boards.

Figure 2 shows the relevant hardware deployed in the experimental facility. The EMC is implemented on a Linux computer, and the GT-based DR algorithm runs in a Linux-based Matlab2018b environment [31]. A graphical user interface (GUI) was developed to monitor the real-time energy consumption of field devices as shown in Figure 3 and a MySQL Database [32] was adopted for storing the energy-consumption data collected from the field devices, from which data can be fetched by the GUI.

IV. EXPERIMENTAL EVALUATION

Based on the experimental system described above, this section evaluates the feasibility of the established DR management system, as well as the effectiveness of the GT-based DR algorithm in managing the real-time energy consumption of field devices in responding to the hourly RTP.

A. BI-DIRECTIONAL INFORMATION EXCHANGE DURING THE SYSTEM EXECUTION PROCESS

To elucidate the work flow of the established system, Figure 4. illustrates the key information exchanges across the whole system. Basically, the information exchanging

TABLE 3. Configuration parameters.

Device type	Continuous Type						Discrete Type					
ID	Motor1	Motor2	Motor3	Lamp1	Lamp2	Lamp3	Motor4	Motor5	Motor6	Lamp4	Lamp5	Lamp6
Priority (β_i)	2.5	2.8	3.1	3.2	3.4	3.6	3.8	3.85	4.05	4.2	4.45	4.7
Energy demand range	30-120 Wh	30-120 Wh	30-120 Wh	20-56 Wh	20-56 Wh	20-56 Wh	75 Wh	75 Wh	75 Wh	35 Wh	35 Wh	35 Wh
Weight (ω)	0.07 (off-peak 12 a.m. – 6 a.m.), 0.06 (middle peak 7 a.m. – 12 p.m.), 0.05 (peak 1 p.m. – 9 p.m.), 0.06 (middle peak 10 p.m. – 11 p.m.)											

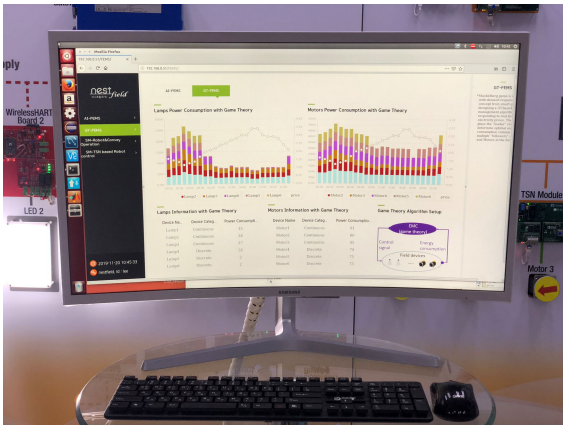

FIGURE 3. Graphical user interface (GUI) of the GT-based DR algorithm in the EMC PC.

process in Figure 4 can be divided into two stages with details specified as follows:

First, during the initialization stage, the EMC firstly tries to build connections with other layers, i.e., an upward connection with the grid-emulating PC and a downward connection with the WirelessHART TCP/IP server and the TSN TCP/IP server on the field layer. As shown on the left side of Figure 4, once the grid server is initiated by the grid-emulating PC, the algorithm client in the EMC will send a request to discover the grid server and then the connection can be built based on the confirmation. Afterwards, the grid-emulating PC will announce a pre-defined RTP program to the EMC (representing a typical DR request sent from the smart grid side), and then the EMC will respond with an acknowledgement of subscribing to the program, in this way the EMC is now regarded to be enrolled in the RTP program and is also ready to receive hourly RTP from the grid-emulating PC. On the right side of Figure 4, the WirelessHART TCP/IP server and the TSN TCP/IP server on the field layer are initiated first, then the TCP/IP client in the EMC tries to discover both servers and build the connection accordingly.

Second, during the execution stage, based on the well-established communication links, each time when EMC receives a new hourly RTP published by the grid-emulating PC, EMC will run the GT-based DR algorithm to generate a new control strategy according to the steps specified in Table 2. The running time for obtaining the control

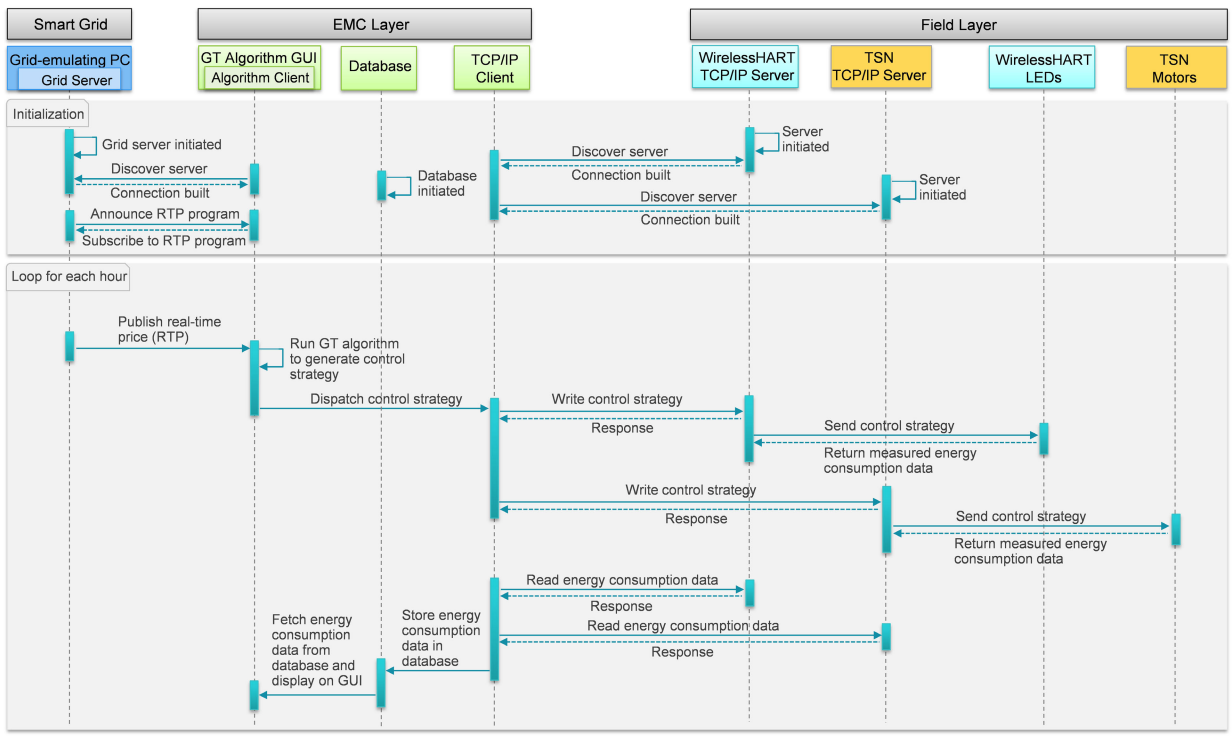

FIGURE 4. Bi-directional information exchange during the system execution process.

TABLE 4. Optimal "on" and "off" States of Discrete Devices.

Discrete type Devices	Hour																							
	00	01	02	03	04	05	06	07	08	09	10	11	12	13	14	15	16	17	18	19	20	21	22	23
Motor 4	1	1	1	1	1	1	1	1	1	1	1	1	1	1	1	1	1	1	1	1	1	1	1	1
Motor 5	1	1	1	1	1	1	1	1	1	1	1	1	1	1	1	1	1	1	0	1	1	1	1	1
Motor 6	1	1	1	1	1	1	1	1	1	1	0	0	0	0	0	0	0	0	0	0	0	0	0	1
Lamp 4	1	1	1	1	1	1	1	1	1	0	0	0	0	0	0	0	0	0	0	0	0	0	0	1
Lamp 5	1	1	1	1	1	1	1	0	0	0	0	0	0	0	0	0	0	0	0	0	0	0	0	0
Lamp 6	0	1	1	1	1	1	1	0	0	0	0	0	0	0	0	0	0	0	0	0	0	0	0	0

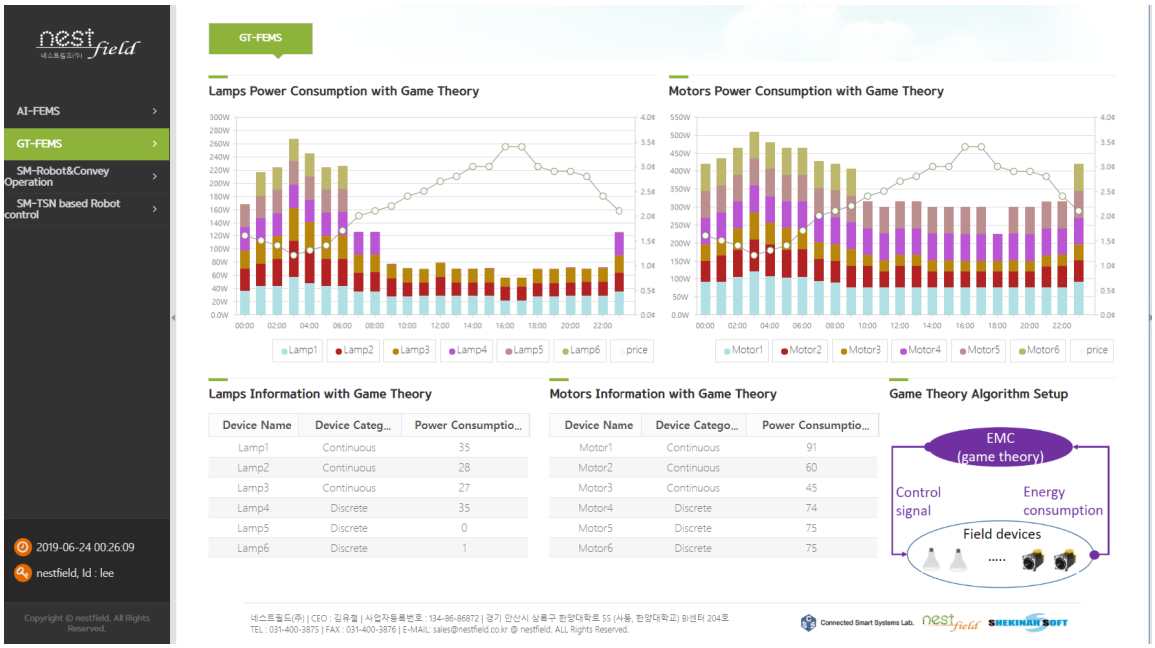

FIGURE 5. Real-time energy consumption monitored using the GUI.

strategy was around 59 ms, such a short computation time can fully meet the requirement of real-time DR in a smart grid application. Afterwards, the obtained control strategy will be dispatched from the EMC to the field level. The procedure for forwarding a message from the EMC to the field devices is depicted in Figure 4, together with the sub-process of returning the measured energy-consumption data from the field devices to the EMC. Note that for the bi-directional communication between the EMC and field devices, the information is always exchanged through two servers placed on the edge of field layer, i.e., the WirelessHART TCP/IP server and the TSN TCP/IP server. In addition, the database on the EMC layer will be updated each hour according to the latest received energy consumption data, which will then be displayed in the GUI in real time, as shown in Figure 3. The experimental evaluation results will be discussed in the next subsection.

B. PERFORMANCE OF GT-bASED DR MANAGEMENT

Based on the experimental facility setup above, the GT-based DR algorithm was tested to verify the DR performance from a practical point of view. Figure 5 shows the hourly power consumption data (i.e., read from the MySQL Database) of the twelve field devices; the upper-left and upper-right figures respectively illustrate the power consumption of the six LED lamps and the six motors with respect to the hourly RTP. Note that for either lamps or motors, the first three devices were continuous type and the other three were discrete type, in line with Table 3. Herein, a discrete type lamp or motor has a constant power when being turned on. At bottom left the exact power consumption of each lamp or motor for a particular instance is shown (i.e., 2019-06-24 00:26:09 in this screen-captured figure). At bottom right, the interactions between the EMC and the field devices are briefly depicted, wherein the control signal is dispatched from the EMC to manage the operations of the field devices, and then the energy consumption data of each device is returned to the EMC for display in the GUI. Next, the DR performance was validated from two aspects.

First, the energy consumption of each device was well controlled in response to the hourly RTP, i.e., devices consumed more energy during off-peak hours when RTPs were low (00:00 – 6:00), and during peak time with extremely high RTPs (14:00 – 18:00), the energy consumption of all

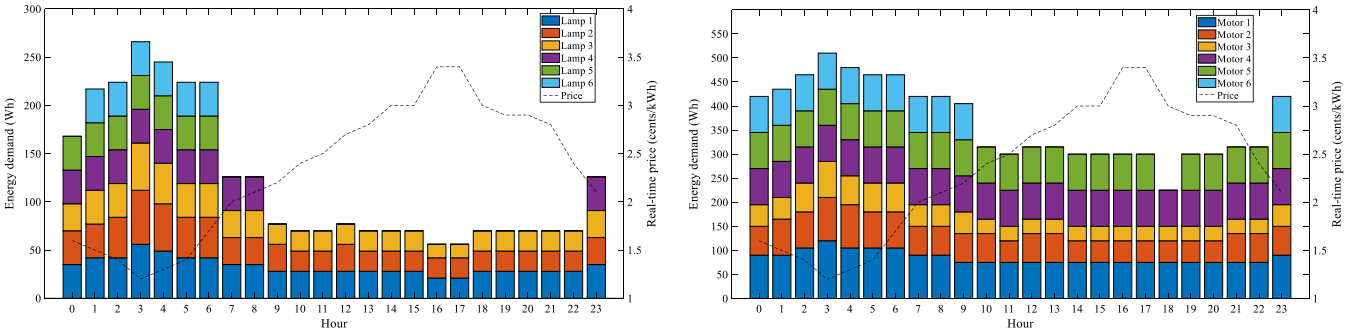

FIGURE 6. Optimal energy demands obtained from the simulation.

the continuous-type devices was reduced significantly or even reduced to the minimum (e.g., Motor 3 and Lamp 3), and discrete-type devices with lower priorities were shut off in response to high RTPs. To have a more intuitive understanding, Table 4 illustrates the optimal "on" and "off" states of discrete type devices, wherein "1" represents "on" and "0" indicates "off". Clearly, the "on/off" states of all the six discrete type devices were appropriately controlled in responding to the dynamic RTPs. Specifically, in face of higher RTPs, devices with lowest priorities were turned off first, e.g., Lamp 6 was off at 00:00, and both Lamp 5 and Lamp 6 were turned off at 07:00. By aggregating the energy consumption of all the devices for each hour, the peak-to-average ratio (PAR) was calculated to be 1.59 according to the following equation [33]:

$$\mathrm{PAR} = \frac{H \max l_h}{\sum_{h=1}^{H} l_h} \tag{9}$$

where $l_h = \sum_{i=1}^{|\mathrm{I}_{con}|} x_i + \sum_{j=1}^{|\mathrm{I}_{dis}|} x_j \cdot x_j^{nom}$ denotes the total energy consumption of all the devices during hour h, and H is the scheduling horizon (i.e., $H = 24$ in the present paper).

Second, the established GT-based DR management system was verified as being able to execute the control strategy appropriately across diverse system components as well as multiple protocols. To elucidate this second aspect fully, Figure 6 shows the energy demands corresponding to the optimal control strategy obtained from the simulation. The operating state of each device in Figure 5 (i.e., experimental results) was consistent with that in Figure 6 (i.e., simulation results), confirming that the established DR management system was able to successfully carry out the real-time control strategy from the EMC layer to the field devices in the correct way. In addition, from Figure 5 and Figure 6, the daily energy cost measured from the experiment was calculated to be \$0.24 and that from the simulation was \$0.25, a negligible difference, which further confirms that the established experimental facility was able to execute the control strategy generated by the GT-based DR algorithm accurately. It can therefore be concluded that through the established experimental facility, the GT-based DR algorithm was verified to be highly effective in practical DR management, which opens up opportunities for more extensive implementations of existing or innovative GT-based DR approaches in diverse application environments.

V. CONCLUSION AND FUTURE WORKS

Upon discovering the research gap between theoretical studies and practical deployment, this work aimed to examine the feasibility of deploying GT-based approaches for practical demand response management. We firstly constructed a pioneering DR-oriented experimental facility by specifying all key techniques, and then provided guidelines to show how to implement a GT-based DR algorithm in such a practical facility. Afterwards, the effectiveness of managing the real-time energy consumption of various field devices was assessed. Based on the experimental results, we concluded that the GT-based algorithm was able to achieve optimal load control and peak load reduction in practical DR management, which can promote more extensive implementations of GT-related DR approaches in diversified DR applications.

In future, the established experimental facility can serve as a base to help evaluate the feasibility of many other kinds of price-based DR approaches, especially those modeled by GT; moreover, the facility can be further developed to support the implementation of incentive-based DR approaches, and can also be easily expanded to deploy more residential devices (e.g., air conditioner, water heater, etc.) as the end devices, since the communication links from top layer to bottom layer have already been well established. In addition, the present GT-based DR approach can be augmented to improve the hourly decision-making with the aid of supervised learning. For instance, the future electricity prices can be predicted through supervised learning algorithm based on the accumulated prices, energy consumption data and weather forecast information. Afterwards, the prediction results can be leveraged by the GT-based DR method to make a more intelligent real-time decision considering both the present and future electricity prices.

APPENDIX A
GAMING PROCESS BETWEEN EMC (LEADER) AND DEVICES (FOLLOWERS)

Given the 1-leader, N-follower Stackelberg game established between the EMC (leader) and devices (followers), the game is played according to a series of consecutive steps [24]:

a) Leader Starts First by Announcing Its Strategy to Followers:

The game is initiated by the leader, who announces its leader strategy (a series of VRPs $\bar{\mathbf{c}} = [c_1, c_2, \ldots, c_N]$) to the followers.

b) Followers Choose Their Best-Response Strategies:

When provided with the leader's strategy ($\bar{\mathbf{c}} = [c_1, c_2, \ldots, c_N]$), each follower i then chooses its best response strategy ($x_i(\bar{\mathbf{c}})$) in response to $\bar{\mathbf{c}}$, here, $x_i(\bar{\mathbf{c}})$ is determined by solving problem (1):

$$x_i(\bar{\mathbf{c}}) = \arg\min_{x_i \in \Omega_i} \mathrm{U}_i(\bar{\mathbf{c}}, x_i) \tag{A.1}$$

where Ω_i denotes the feasible strategy set of follower i constructed by constraint (1c) or (1d), depending on the type of device.

c) Leader Chooses Its Optimal Strategy Based on the Identified Best-Response Strategies of Followers:

Based on the identified best-response strategy of each follower, i.e., $x_1(\bar{\mathbf{c}}), \ldots, x_N(\bar{\mathbf{c}})$, the leader will then choose an optimal strategy $\bar{\mathbf{c}}^*$ by solving problem (3):

$$\bar{\mathbf{c}}^* = \arg\max_{\bar{\mathbf{c}} \in \Omega_{EMC}} U_{EMC}(\bar{\mathbf{c}}, x_1(\bar{\mathbf{c}}), \ldots, x_N(\bar{\mathbf{c}})) \tag{A.2}$$

where Ω_{EMC} denotes the feasible strategy set of the leader constructed by constraint (3b) and (3c).

d) Repeat a)-c) to Obtain the Desired Outcome of the Game

Once an optimal strategy is chosen by the leader in step *c*), the leader will announce it to followers again. In this manner, the process from *a*) to *c*) is repeated between the EMC and devices until the desired outcome is obtained.

It is worth noting that the gaming process described above aims to illustrate the inherency of the virtual trading procedure between the EMC and devices. In Part *D* of Section II, we showed that a unique and optimal Stackelberg Equilibrium (SE) was proven to exist in the formulated 1-leader, N-follower game between the EMC and the devices. Moreover, the SE can be directly derived using backward induction [24], avoiding iterations, which could significantly reduce the computational time required for this GT-based DR algorithm.

APPENDIX B
PROOF OF THE STRICIT CONVEXITY OF THE REFORMULATED OPTIMIZATION PROBLEM

Clearly, the reformulated objective function in (8a) composes of two parts, i.e., the part related with continuous type devices and the part related with discrete type devices. Note that the convexity of the case when only the first part is involved has been well proven by work [24] (refer to Part *C* of Section III in [24]). Therefore, herein we only need to prove the convexity when discrete type devices are involved, and the proof is given as follows.

For a discrete energy-demand device i, we first relax the binary decision variable x_i to a real-valued variable, $0 \le x_i \le 1$. Afterwards, the best-response function can be directly obtained by taking the first-order derivative of $\mathrm{U}_i(\bar{\mathbf{c}}, x_i)$ in terms of (1b) with respect to x_i (note that the dissatisfaction cost $\varphi_i(\cdot)$ in (1b) takes the form of (2b)):

$$\frac{\partial \mathrm{U}_i(\bar{\mathbf{c}}, x_i)}{\partial x_i} = c_i \cdot x_i^{nom} - \frac{\omega \beta_i}{\tau_i} \cdot e^{\beta_i\left(1-(\frac{x_i}{\tau_i})\right)} \tag{B.1}$$

By taking (B.1) to be zero, we obtain the best-response function as follows:

$$x_i(\bar{\mathbf{c}}) = \tau_i\left(1 - \frac{1}{\beta_i} \ln \frac{c_i x_i^{nom} \tau_i}{\omega \beta_i}\right) \tag{B.2}$$

In addition, the second-order derivative of $\mathrm{U}_i(\bar{\mathbf{c}}, x_i)$ is calculated to be

$$\frac{\partial^2 \mathrm{U}_i(\bar{\mathbf{c}}, x_i)}{\partial x_i^2} = \frac{\omega {\beta_i}^2}{\tau_i^2} e^{\beta_i(1-\frac{x_i}{\tau_i})} \tag{B.3}$$

Obviously, the value of (B.3) is always positive such that $\mathrm{U}_i(\bar{\mathbf{c}}, x_i)$ is strictly convex at x_i, indicating the best-response strategy obtained by (B.2) is unique and optimal.

Next, we substitute (B.2) into the EMC utility function in (3a) by considering discrete type devices only, then, $\mathrm{U}_{EMC}(\bar{\mathbf{c}}, \bar{\mathbf{x}})$ can be rewritten as follows:

$$\begin{aligned}
&\mathrm{U}_{EMC}(\bar{\mathbf{c}}, \bar{\mathbf{x}}) \\
&= \sum\nolimits_{i=1}^{|\mathbf{I}_{\mathrm{dis}}|} c_i x_i(\bar{\mathbf{c}}) - \sum\nolimits_{i=1}^{|\mathbf{I}_{\mathrm{dis}}|} \omega \cdot \varphi_i(x_i(\bar{\mathbf{c}})) \\
&= \sum\nolimits_{i=1}^{|\mathbf{I}_{\mathrm{dis}}|} \left(c_i \cdot \tau_i\left(1 - \frac{1}{\beta_i} \ln \frac{c_i x_i^{nom} \tau_i}{\omega \beta_i}\right)\right) \\
&\quad - \sum\nolimits_{i=1}^{|\mathbf{I}_{\mathrm{dis}}|} \left(\frac{c_i x_i^{nom} m_i}{\beta_i} - \omega\right)
\end{aligned} \tag{B.4}$$

The Hessian matrix of $\mathbf{U}_{EMC}(\bar{\mathbf{c}}, \bar{\mathbf{x}})$ in (B.4) can be calculated by taking the second derivative of $\mathbf{U}_{EMC}(\bar{\mathbf{c}}, \bar{\mathbf{x}})$ with respect to c_i. We then obtain

$$\frac{\partial^2 \mathrm{U}_{EMC}(\bar{\mathbf{c}}, \bar{\mathbf{x}})}{\partial c_i \partial c_j} = \begin{cases} -\frac{\tau_i}{c_i \cdot \beta_i} & when\ j = i \\ 0 & when j \ne i \end{cases} \tag{B.5}$$

Therefore, the Hessian matrix of $\mathrm{U}_{EMC}(\bar{\mathbf{c}}, \bar{\mathbf{x}})$ is still *strictly negative definite*, implying that $\mathrm{U}_{EMC}(\bar{\mathbf{c}}, \bar{\mathbf{x}})$ is strictly concave in the feasible region of $\bar{\mathbf{c}}$. Moreover, it deserves noticing that the exponential terms in constraints (7a) and (7b) will finally turn to constants since all the symbols are parameters, in other words, there is no variable "x_i" in constraints. Therefore, (7a) and (7b) are convex constraints. Consequently, the reformulated optimization problem expressed in (8a) and (8b) are proven to be a standard convex problem, meaning that a unique and optimal solution can be guaranteed accordingly to Theorem 1 in [24]. To this end, the proof of the convexity of the reformulated optimization problem is completed.

APPENDIX C
OPTIMAL VIRTUAL RETAIL PRICE (VRP) DETERMINED FOR EACH DEVICE

For the GT-based DR algorithm, VRP acts as an intermediate tool for deriving the optimal control strategy. After executing the command of Step 4 in Table 2, optimal VRPs can be determined for each device. As shown in Figure 7, for each

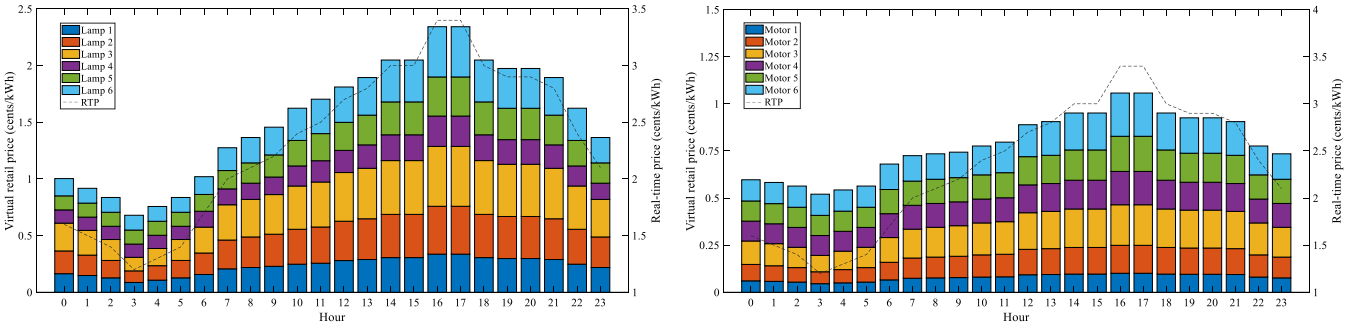

FIGURE 7. Optimal virtual retail price (VRP) for each device.

hour, the sum of VRPs for all the twelve devices equals to the RTP during that hour. Moreover, the VRP for a lower priority (greater β_i) device (e.g., Motor 2) was determined to be higher than that of a higher priority (smaller β_i) device (e.g., Motor 1). As a result, Motor 2 demanded less energy than Motor 1 (refer to Figure 6) since the EMC charged higher VRP to Motor 2. Based on the obtained VRPs for each device, the optimal control strategy can be determined by executing Step 5 in Table 2, which will be used for managing the energy consumption of all the field devices.

REFERENCES

[1] N. G. Paterakis, O. Erdinç, and J. P. S. Catalao, "An overview of demand response: Key-elements and international experience," *Renew. Sustain. Energy Rev.*, vol. 69, pp. 871–891, Mar. 2017, doi: 10.1016/j.rser.2016.11.167.

[2] Z. Xu, T. Deng, Z. Hu, Y. Song, and J. Wang, "Data-driven pricing strategy for demand-side resource aggregators," *IEEE Trans. Smart Grid*, vol. 9, no. 1, pp. 57–66, Jan. 2018, doi: 10.1109/TSG.2016.2544939.

[3] D. Liu, Y. Sun, Y. Qu, B. Li, and Y. Xu, "Analysis and accurate prediction of user's response behavior in incentive-based demand response," *IEEE Access*, vol. 7, pp. 3170–3180, 2019, doi: 10.1109/ACCESS.2018.2889500.

[4] S. Zheng, Y. Sun, B. Li, B. Qi, K. Shi, Y. Li, and X. Tu, "Incentive-based integrated demand response for multiple energy carriers considering behavioral coupling effect of consumers," *IEEE Trans. Smart Grid*, vol. 11, no. 4, pp. 3231–3245, Jul. 2020, doi: 10.1109/TSG.2020.2977093.

[5] L. Jia and L. Tong, "Dynamic pricing and distributed energy management for demand response," *IEEE Trans. Smart Grid*, vol. 7, no. 2, pp. 1128–1136, Mar. 2016, doi: 10.1109/TSG.2016.2515641.

[6] D. Liu, Y. Sun, B. Li, X. Xiangying, and L. Yudong, "Differentiated incentive strategy for demand response in electric market considering the difference in user response flexibility," *IEEE Access*, vol. 8, pp. 17080–17092, 2020, doi: 10.1109/ACCESS.2020.2968000.

[7] R. Tang, S. Wang, and H. Li, "Game theory based interactive demand side management responding to dynamic pricing in price-based demand response of smart grids," *Appl. Energy*, vol. 250, pp. 118–130, Sep. 2019, doi: 10.1016/j.apenergy.2019.04.177.

[8] T. Hahn, Z. Tan, and W. Ko, "Design of time-varying rate considering CO_2 emission," *IEEE Trans. Smart Grid*, vol. 4, no. 1, pp. 383–389, Mar. 2013, doi: 10.1109/TSG.2012.2234771.

[9] A. Safdarian, M. Fotuhi-Firuzabad, and M. Lehtonen, "Optimal residential load management in smart grids: A decentralized framework," *IEEE Trans. Smart Grid*, vol. 7, no. 4, pp. 1836–1845, Jul. 2016, doi: 10.1109/TSG.2015.2459753.

[10] Z. Zhu, S. Lambotharan, W. H. Chin, and Z. Fan, "A game theoretic optimization framework for home demand management incorporating local energy resources," *IEEE Trans. Ind. Informat.*, vol. 11, no. 2, pp. 353–362, Apr. 2015, doi: 10.1109/TII.2015.2390035.

[11] C. Chen, S. Kishore, and L. V. Snyder, "An innovative RTP-based residential power scheduling scheme for smart grids," presented at the IEEE Int. Conf. Acoust., Speech Signal Process. (ICASSP), May 2011.

[12] X. Xue, S. Wang, C. Yan, and B. Cui, "A fast chiller power demand response control strategy for buildings connected to smart grid," *Appl. Energy*, vol. 137, pp. 77–87, Jan. 2015, doi: 10.1016/j.apenergy.2014.09.084.

[13] D. Murayama, K. Mitsumoto, Y. Takagi, Y. Iino, and S. Yamamori, "Smart grid ready BEMS adopting model-based HVAC control for energy saving," in *Proc. PES T D*, May 2012, pp. 1–6, doi: 10.1109/TDC.2012.6281521.

[14] Z. Luo, S. H. Hong, and J.-B. Kim, "A price-based demand response scheme for discrete manufacturing in smart grids," *Energies*, vol. 9, no. 8, p. 650, Aug. 2016, doi: 10.3390/en9080650.

[15] Y. M. Ding, S. H. Hong, and X. H. Li, "A demand response energy management scheme for industrial facilities in smart grid," *IEEE Trans. Ind. Informat.*, vol. 10, no. 4, pp. 2257–2269, Nov. 2014, doi: 10.1109/TII.2014.2330995.

[16] M. Yu, S. H. Hong, Y. Ding, and X. Ye, "An incentive-based demand response (DR) model considering composited DR resources," *IEEE Trans. Ind. Electron.*, vol. 66, no. 2, pp. 1488–1498, Feb. 2019, doi: 10.1109/TIE.2018.2826454.

[17] W. Saad, Z. Han, H. Poor, and T. Basar, "Game-theoretic methods for the smart grid: An overview of microgrid systems, demand-side management, and smart grid communications," *IEEE Signal Process. Mag.*, vol. 29, no. 5, pp. 86–105, Sep. 2012, doi: 10.1109/MSP.2012.2186410.

[18] L. Ma, N. Liu, J. Zhang, W. Tushar, and C. Yuen, "Energy management for joint operation of CHP and PV prosumers inside a grid-connected microgrid: A game theoretic approach," *IEEE Trans. Ind. Informat.*, vol. 12, no. 5, pp. 1930–1942, Oct. 2016, doi: 10.1109/TII.2016.2578184.

[19] S. Zheng, Y. Sun, B. Li, B. Qi, K. Shi, Y. Li, and Y. Du, "Bargaining-based cooperative game among multi-aggregators with overlapping consumers in incentive-based demand response," *IET Gener., Transmiss. Distrib.*, vol. 14, no. 6, pp. 1077–1090, Mar. 2020, doi: 10.1049/iet-gtd.2019.1084.

[20] M. Yu, S. H. Hong, X. Zhang, J. Jiang, X. Huang, M. Wei, K. Wang, and W. Liang, "Incentivizing strategy for demand response aggregator considering market entry criterion: A game theoretical approach," in *Proc. IEEE 17th Int. Conf. Ind. Informat. (INDIN)*, Jul. 2019, pp. 1077–1082, doi: 10.1109/INDIN41052.2019.8972269.

[21] H. Alsalloum, L. Merghem-Boulahia, and R. Rahim, "Hierarchical system model for the energy management in the smart grid: A game theoretic approach," *Sustain. Energy, Grids Netw.*, vol. 21, Mar. 2020, Art. no. 100329, doi: 10.1016/j.segan.2020.100329.

[22] Y. Jiang, K. Zhou, X. Lu, and S. Yang, "Electricity trading pricing among prosumers with game theory-based model in energy blockchain environment," *Appl. Energy*, vol. 271, Aug. 2020, Art. no. 115239, doi: 10.1016/j.apenergy.2020.115239.

[23] S. Teimourzadeh, O. B. Tor, M. E. Cebeci, A. Bara, S. V. Oprea, and S. M. Kisakurek, "Enlightening customers on merits of demand-side load control: A simple-but-efficient-platform," *IEEE Access*, vol. 8, pp. 193238–193247, 2020, doi: 10.1109/ACCESS.2020.3032745.

[24] M. Yu and S. H. Hong, "A real-time demand-response algorithm for smart grids: A Stackelberg game approach," *IEEE Trans. Smart Grid*, vol. 7, no. 2, pp. 879–888, Mar. 2016, doi: 10.1109/TSG.2015.2413813.

[25] M. J. Osborne and A. Rubinstein, *A Course in Game Theory*. Cambridge, MA, USA: MIT Press, 1994.

[26] *Industrial Communication Networks—Wireless Communication Network and Communication Profiles—WirelessHART*, document IEC 62591, 2010.

[27] *Time-Sensitive Networking Task Group*. Accessed: Dec. 15, 2020. [Online]. Available: http://www.ieee802.org/1/pages/tsn.html
[28] *Raspberry Pi Documentation*. Accessed: Dec. 15, 2020. [Online]. Available: https://www.raspberrypi.org/documentation/
[29] *Commonwealth Edison Company. Real-Time Hourly Prices*. Accessed: Dec. 15, 2020. [Online]. Available: https://rrtp.comed.com/live-prices/
[30] *OpenADR 2.0 Specifications*. Accessed: Dec. 15, 2020. [Online]. Available: https://www.openadr.org/specification
[31] *Start MATLAB on Linux Platforms*. Accessed: Dec. 15, 2020. [Online]. Available: https://www.mathworks.com/help/matlab/matlab_env/start-matlab-on-linux-platforms.html
[32] *MySQL Database*. Accessed: Dec. 15, 2020. [Online]. Available: https://www.mysql.com/downloads/
[33] A.-H. Mohsenian-Rad, V. W. S. Wong, J. Jatskevich, R. Schober, and A. Leon-Garcia, "Autonomous demand-side management based on game-theoretic energy consumption scheduling for the future smart grid," *IEEE Trans. Smart Grid*, vol. 1, no. 3, pp. 320–331, Dec. 2010, doi: 10.1109/TSG.2010.2089069.

MENGMENG YU (Member, IEEE) received the B.S. degree in communication engineering from the Wuhan University of Technology, Wuhan, China, in 2008, the M.S. degree in detection technique and automation equipment from the Chongqing University of Posts and Telecommunications, Chongqing, China, in 2011, and the Ph.D. degree in electronic systems engineering from Hanyang University, Ansan, South Korea, in 2015.

From 2015 to 2018, she was a Postdoctoral Researcher under the BK21 PLUS Program (BK21+) with Hanyang University, where she is currently a Research Assistant Professor with the Research Institute of Engineering and Technology. Her research interests include smart grid, game theory, artificial intelligence, and smart manufacturing. She was a recipient of the Outstanding Researcher Award of BK21+ and the Best Paper Award from the Workshop on Smart City Infrastructure and Applications, in 2016.

XIONGFENG ZHANG received the B.S. degree in automation from the Wuhan University of Science and Technology, Wuhan, China, in 2016. He is currently pursuing the Ph.D. degree with the Department of Electronic Systems Engineering, Hanyang University, Ansan, South Korea.

His research interests include artificial intelligence, demand response in smart grid, cyber physical systems, and smart manufacturing.

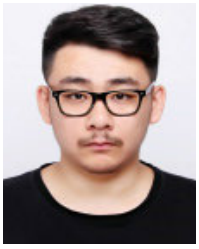

JUNHUI JIANG (Graduate Student Member, IEEE) received the B.S. degree in electronic information engineering from the Harbin University of Science and Technology, Harbin, China, in 2017. He is currently pursuing the Ph.D. degree with the Department of Electronic Systems Engineering, Hanyang University, Ansan, South Korea. His research interests include routing and scheduling algorithms, performance evaluation, and run-time configuration for the deterministic real-time networks. He is a member of the IEEE Industrial Electronics Society. He was a recipient of the Young Professionals Award from the IEEE International Conference on Emerging Technologies and Factory Automation, in 2019.

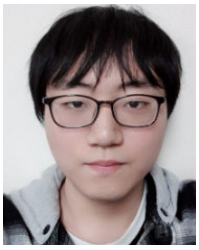

CHANGDAE LEE (Student Member, IEEE) received the B.S. degree in electronic engineering from Kangwon National University, South Korea, in 2017. He is currently pursuing the Ph.D. degree in electronic engineering with Hanyang University, Ansan, South Korea. His research interests include reliability, performability, communication protocols for industrial control and automation, industrial informatics, and wireless communication protocols.

SEUNG HO HONG (Senior Member, IEEE) received the B.S. degree from Yonsei University, Seoul, South Korea, in 1982, the M.S. degree from Texas Tech University, Lubbock, TX, USA, in 1985, and the Ph.D. degree from Pennsylvania State University, University Park, in 1989, all in mechanical engineering.

He is currently a Professor with the Department of Electronic Engineering and the Director of the Connected Smart Systems Laboratory, Hanyang University, Ansan, South Korea. He was a Visiting Scholar with the U.S. National Institute of Standards and Technology, the Vienna University of Technology, Austria, and the Zhejiang University, China. He is also a Foreign Expert with the Tianjin University of Technology through the Tianjin Thousand Talents Program. His research interests include smart manufacturing, smart grid, the Industrial Internet of Things, cyberphysical systems, and artificial intelligence. He is a member of the IEEE Industrial Electronics Society and the International Electrotechnical Commission System Committee Smart Manufacturing.

KAI WANG received the Ph.D. degree in mechatronic engineering from the Shenyang Institute of Automation (SIA), Chinese Academy of Sciences (CAS).

He was a Visiting Scholar with the Center for Advanced Life Cycle Engineering (CALCE), University of Maryland, from 2014 to 2016. He is currently an Associate Professor with SIA, CAS. He is also a Tutor for graduate with the University of CAS. He has over 50 publications. His primary research interests include industrial artificial intelligence, fault diagnosis, prognostics and health management, and reliability engineering. He is specially focused on degradation mechanisms of electromagnetic coil insulation and methods to detect degraded insulation prior to the formation of shorts in electromagnetic coils. He received the Best Academic Presentation Award from the 2013 IEEE International Conference on Electronic Measurement and Instruments.

AIDONG XU received the M.E. degree in computer science from Northeast University, in 1998, and the Ph.D. degree in electromechanical engineering from the Shenyang Institute of Automation (SIA), Chinese Academy of Sciences, in 2012. His research interests include industrial digital communications, cyber security, and reliability.

He is currently a Research Fellow with SIA. He is a member of the International Electrotechnical Commission/Industrial Process Measurement and Control Committee/Industrial Network (IEC/TC65/SC65C).